

Model of Centauro and strangelet production in heavy ion collisions

A. L. S. Angelis,¹ E. Gładysz-Dziaduś,² Yu. V. Kharlov,³ V. L. Korotkikh,⁴
G. Mavromanolakis,¹ A. D. Panagiotou,¹ and S. A. Sadovsky³

¹*Nuclear and Particle Physics Division,*

Physics Department, University of Athens, Athens, Greece

²*Laboratory of High Energy Physics, Institute of Nuclear Physics, Krakow, Poland*

³*Institute for High Energy Physics, Protvino, Russia*

⁴*Moscow State University, SINP, Moscow, Russia*

We discuss the phenomenological model of Centauro event production in relativistic nucleus–nucleus collisions. This model makes quantitative predictions for kinematic observables, baryon number and mass of the Centauro fireball and its decay products. Centauros decay mainly to nucleons, strange hyperons and possibly strangelets. Simulations of Centauro events for the CASTOR detector in $Pb+Pb$ collisions at LHC energies are performed. The signatures of these events are discussed in detail.

Introduction

In this paper we present the Monte Carlo generator of Centauro events [1, 2], produced in relativistic nucleus–nucleus collisions based on the phenomenological model described in [3, 4, 5, 6]. Originally the generator has been used to simulate Centauro production in $\sqrt{s} = 5.5 \times A$ TeV $Pb + Pb$ collisions at the LHC and to study the performance of the CASTOR detector, which was initially under development for the ALICE experiment [7]. Later it became clear that the infrastructure of the experiment CMS [8] is more suitable for these studies and the decision has been taken to carry out this experiment in the CMS.

Originally the model of Centauro event production was based on experimental facts known from the cosmic ray studies. Experimentally observed characteristics such as multiplicities, transverse momenta, energy spectra and pseudorapidity distributions of secondary particles inspired the scenario of the Centauro fireball evolution through which the thermodynamical

parameters and the lifetime of the Centauro fireball can be calculated. The extrapolation of this model to higher energies allowed to estimate some observables of Centauro events at the LHC energy range taking into account the collider kinematics [9].

In the approach adopted here we attempt to predict more precisely the characteristics of such events. We present the quantitative description of the original phenomenological model of Centauro production in nucleus–nucleus collisions under the assumption of some fundamental characteristics of the Centauro fireball, leading to more detailed predictions of observables in such events. The model is formulated in terms of the impact parameter of the nucleus–nucleus collision, two thermodynamical parameters (baryochemical potential and temperature) which are assigned to the Centauro fireball and the nuclear stopping power. In order to construct a fully quantitative model we formalize all assumptions of the original model and introduce some additional ones. The event generator CNGEN calculates the Centauro fireball parameters and produces the full event configuration. In this manner the model reproduces all the kinematical parameters of the Centauro events which were observed in cosmic ray experiments.

In section 1 we give the thermodynamical and kinematical description of the production and evolution of Centauro-type events in relativistic nucleus–nucleus collisions and present some of their characteristics such as their mass, energy and multiplicity distributions.

In section 2 we give results on the detection capability of such events with the CASTOR detector. Centauro events are compared with conventional events produced by the HIJING generator [14]. Signatures of Centauro events are discussed.

I. PHYSICS OF CENTAURO EVENTS

Centauro fireball evolution. The phenomenological description of Centauro events was introduced in [3, 4, 5]. According to this model Centauro events are produced in the projectile fragmentation region of a relativistic nuclear collision when the projectile nucleus penetrating through the target nucleus transforms its kinetic energy to heat and forms a relatively cool quark matter state with high baryochemical potential [4, 5]. We refer to this quark matter state as the primary Centauro fireball. At the first stage of its evolution it contains u and d quarks and gluons. The high baryochemical potential inhibits gluons from fragmenting into $u\bar{u}$ and $d\bar{d}$ pairs due to Pauli blocking [4]. Therefore gluons fragment into

$s\bar{s}$ pairs and a state of partial chemical equilibrium is achieved. During this time \bar{s} quarks couple with u and d quarks and a number of K^+ and K^0 are emitted from the primary fireball, decreasing the temperature and removing entropy. At the end of this stage the Centauro fireball has become a slightly strange quark matter (SQM) fireball with a relatively long lifetime ($\tau \sim 10^{-9}$ sec) [10]. In the case of cosmic ray Centauros this allows the fireball to reach mountain top altitudes. At the same time a mechanism of strangeness separation [11] can cause the strange quark content of the SQM fireball to accumulate in one or more smaller regions inside it. The SQM fireball finally decays explosively into non-strange baryons and light ($A > 6$) strange quark matter objects (strangelets).

Baryon number of the Centauro fireball. We consider collisions of nuclei with atomic numbers A_1 and A_2 and charges Z_1 and Z_2 respectively. The impact parameter b is roughly restricted by

$$0 < b < R_1 + R_2,$$

where $R_i = 1.15A_i^{1/3}$ fm ($i = 1, 2$) are the radii of the colliding nuclei. The Centauro fireball is produced in the region of overlap of the two nuclei. We assume that all nucleons of the projectile nucleus which fall within this region can interact, and that it is these nucleons which define the fireball's baryon number. The baryon number N_b of the fireball can then be estimated from simple geometrical considerations. Assuming a uniform distribution of nucleons in a nucleus one can obtain N_b through the ratio of the volumes of the overlapping region V_{ovrlp} and the whole projectile nucleus V_1 :

$$N_b = 0.9 A_1 \frac{V_{\text{ovrlp}}}{V_1}. \quad (1)$$

Where the factor 0.9 has been introduced in order to exclude the contribution to N_b from the boundaries of the overlapping region.

It is natural to assume that projectile and target nuclei are distributed uniformly in the transverse plane, i.e. that b^2 is distributed uniformly. This assumption determines the shape of further distributions presented below. All cosmic ray Centauro events were observed with hadron multiplicity $N_h > 70$, hence in our model we restrict the Centauro fireball production to $N_b > 50$.

In our quantitative model we use the assumption that each nucleus–nucleus collision produces a Centauro fireball characterized by the same thermodynamical parameters. This assumption is reasonable when only small variations of the impact parameter are considered.

Central collisions are more likely to produce the Centauro fireball than peripheral ones because of the larger baryon content. Therefore the distributions shown in this paper have been calculated for $Pb + Pb$ collisions with impact parameter $0 < b < 5$ fm.

The baryon number distribution of the Centauro fireball produced in $\sqrt{s} = 5.5 \times A$ TeV $Pb + Pb$ collisions is shown in Fig. 1.

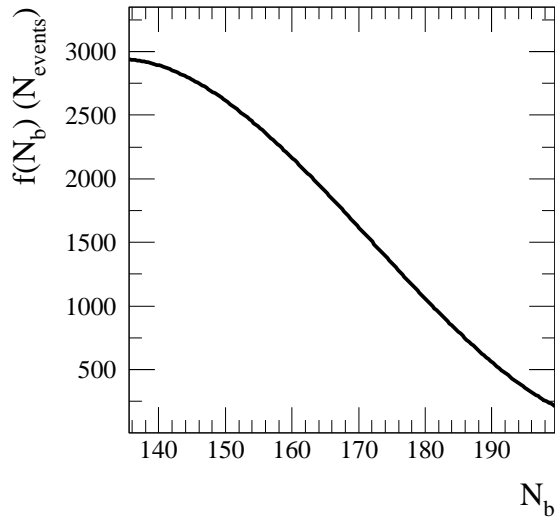


FIG. 1: Baryon number of the Centauro fireball produced in $\sqrt{s} = 5.5 \times A$ TeV $Pb + Pb$ collisions with impact parameter $0 < b < 5$ fm.

Mass of the Centauro fireball. The Centauro fireball is a drop of deconfined quark matter characterized by a temperature T and a baryochemical potential μ_b . As the phenomenological model [4, 5] predicts, it has a very high baryochemical potential which does not permit the production of \bar{u} and \bar{d} antiquarks. This state of the Centauro fireball is unstable and after $\Delta t \sim 10^{-23}$ sec [5] gluons fragment into $s\bar{s}$ pairs and chemical equilibrium in the fireball is achieved. In first-order perturbative QCD the energy density of quark-gluon plasma containing u , d , s quarks and gluons at temperature T close to the critical temperature T_c is expressed by (see e.g. [12, 13] and references therein)

$$\varepsilon = \varepsilon_g + \varepsilon_q + \varepsilon_s.$$

Here $q = u, d$. Gluon and quark contributions ε_g , ε_q and ε_s are

$$\begin{aligned} \varepsilon_g &= \frac{8\pi^2}{15} T^4 \left(1 - \frac{15}{4\pi} \alpha_s \right), \\ \varepsilon_q &= \frac{7\pi^2}{10} T^4 \left(1 - \frac{50}{21\pi} \alpha_s \right) + \left(3\mu_q^2 T^2 + \frac{3}{2\pi^2} \mu_q^4 \right) \left(1 - \frac{2}{\pi} \alpha_s \right), \\ \varepsilon_s &= \gamma_s \left[\left(\frac{18T^4}{\pi^2} \right) \left(\frac{m_s}{T} \right)^2 K_2 \left(\frac{m_s}{T} \right) + 6 \left(\frac{m_s T}{\pi} \right)^2 \left(\frac{m_s}{T} \right) K_1 \left(\frac{m_s}{T} \right) \right]. \end{aligned}$$

Here K_i are i -order modified Bessel functions. The strong coupling constant α_s should be taken at a scale $Q \approx 2\pi T$ and equals $\alpha_s = 0.3$ at a critical temperature $T_c = 170$ MeV [13]. The γ_s is the strangeness equilibration factor ($\gamma_s \approx 0.4$). The net energy density for all degrees of freedom is given by

$$\varepsilon = \frac{37\pi^2}{30}T^4 \left(1 - \frac{110}{37\pi}\alpha_s\right) + \left(3\mu_q^2 T^2 + \frac{3}{2\pi^2}\mu_q^4\right) \left(1 - \frac{2}{\pi}\alpha_s\right) + \varepsilon_s. \quad (2)$$

Here the quark chemical potential μ_q can be expressed via the baryochemical potential μ_b as $\mu_q = \mu_b/3$.

The other thermodynamical quantities of interest, pressure P and quark number density $n_q = N_q/V_{\text{fb}}$ are obtained from equation (2):

$$P = \frac{1}{3}\varepsilon, \quad n_q = \left(\frac{\partial P}{\partial \mu_q}\right)_T, \\ n_q = 2 \left(\mu_q T^2 + \frac{\mu_q^3}{\pi^2}\right) \left(1 - \frac{2}{\pi}\alpha_s\right). \quad (3)$$

Since the number of quarks N_q in the primary Centauro fireball is defined from the collision geometry as $N_q = 3N_b$ one can obtain from (1) and (3) the volume of the fireball V_{fb} to order $\mathcal{O}(\alpha_s)$:

$$V_{\text{fb}} = \frac{3N_b}{2 \left(\mu_q T^2 + \frac{\mu_q^3}{\pi^2}\right)} \left(1 + \frac{2}{\pi}\alpha_s\right). \quad (4)$$

When the volume of the fireball is defined one can easily obtain the mass of the fireball from the energy density (2):

$$M_{\text{fb}} = \varepsilon V_{\text{fb}}. \quad (5)$$

The distribution of the Centauro fireball mass produced in $\sqrt{s} = 5.5 \times A$ TeV $Pb + Pb$ collisions with $\mu_b = 1.8$ GeV and $T = 130, 190$ and 250 MeV is shown in Fig. 2

Kinematics of the Centauro fireball. Centauro events were observed in cosmic ray experiments in the very forward region [1, 2]. We assume that the longitudinal momentum distribution of the Centauro fireball obeys the same scaling law of secondary particle production described by the empirical formula established at lower energies for large x_F :

$$dN/dx_F \sim (1 - x_F)^n, \quad n \approx 3.$$

Each constituent quark of the projectile nucleus which participates in the formation of the fireball undergoes scattering by the target nucleus. The transverse momentum distribution

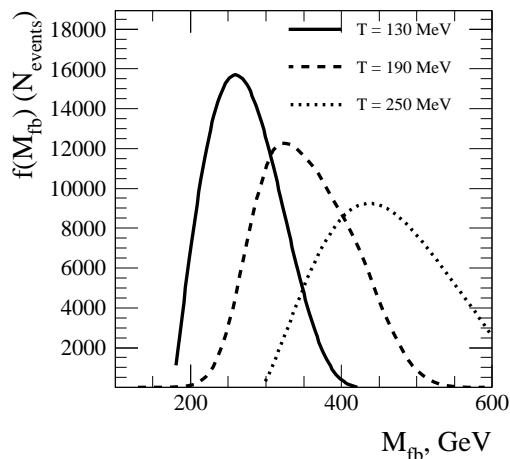


FIG. 2: Mass of the Centauro fireball produced in $\sqrt{s} = 5.5 \times A$ TeV $Pb+Pb$ collisions with $\mu_b = 1.8$ GeV and $T = 130, 190$ and 250 MeV.

of a quark in the fragmentation region can be expressed by the form

$$dN_q/dp_T^2 \sim \exp\left(-\frac{p_T^2}{p_0^2}\right)$$

with the slope $p_0 = 0.3$ GeV/ c . Vector summation of the transverse momenta of all interacting quarks gives the transverse momentum of the produced Centauro fireball.

The rapidity range of the fireball can be obtained from the following consideration. The maximum rapidity of the fireball is reached when it carries the full energy of the overlapping part of the projectile nucleus, $E_{\max} = E_{\text{beam}} N_b / A_{\text{beam}}$:

$$y_{\max} = \ln \frac{2E_{\max}}{M_{\text{fb}}}.$$

For example for central $Pb+Pb$ collisions at $\sqrt{s} = 5.5 \times A$ TeV and $N_b = 0.9 A_{\text{beam}} = 186$, assuming $T = 190$ MeV and $\mu_b = 1.8$ GeV, one obtains the fireball mass $M_{\text{fb}} = 466$ GeV/ c^2 and the maximum rapidity is

$$y_{\max} = 7.69.$$

However the nuclear stopping has to be considered as well, as it is an important effect in heavy ion collisions. It embodies the degree to which the energy of relative motion of the two incident nuclei can be transferred into thermodynamical degrees of freedom. The nuclear stopping can be expressed through the rapidity shift $\Delta y_{\text{n.s.}}$ of produced particles compared to the maximum rapidity in NN collisions. The actual rapidity of the Centauro fireball is therefore defined by the equation

$$y_{\text{fb}} = y_{\max} - \Delta y_{\text{fb}}. \quad (6)$$

The value of Δy_{fb} is related to $\Delta y_{\text{n.s.}}$ and is a crucial input parameter of the model on which the observation of the Centauro events depends. The average of the HIJING [14] and VENUS [15] predictions gives $\Delta y_{\text{n.s.}} = 2.3$ but values in the range $2.0 < \Delta y_{\text{n.s.}} < 3.5$ can occur [5].

Recoil system. Once the kinematics of the fireball are defined one can calculate the momentum of the recoil system which consists of secondaries from the target nucleus. Defining the 4-momentum of the Centauro fireball as p_{Cn} and the 4-momentum of the recoil system as p_{rec} we have the momentum conservation law as

$$p_{\text{proj}} + p_{\text{targ}} = p_{\text{Cn}} + p_{\text{rec}}.$$

Let $\sqrt{s_{aa}}$ be the c.m.s. collision energy of the overlapping fragments of the beam nuclei. If $\sqrt{s_{NN}}$ is the collision energy per nucleon we obviously have $\sqrt{s_{aa}} = N_b \sqrt{s_{NN}}$ with N_b defined by equation (1). Neglecting the mass of the Centauro fireball in comparison with $\sqrt{s_{aa}}$ we obtain the mass of the recoil system M_{rec} to be defined by the expression

$$M_{\text{rec}} = \sqrt{s_{aa}}(1 - \delta)^{1/2},$$

where $\delta \approx 2M_{\text{fb}} \cosh(y_{\text{fb}})/\sqrt{s_{aa}}$. For the rapidity of the recoil system y_{rec} the equation is as follows:

$$\sinh y_{\text{rec}} \approx \frac{\delta/2}{(1 - \delta)^{1/2}}.$$

For values of the fireball rapidity shift Δy_{fb} of several units, $\Delta y_{\text{fb}} = 2 - 3$, one can conclude that the recoil system carries almost the total energy $\sqrt{s_{aa}}$ of the nuclear collision. In this approximation it is easy to show that δ vanishes, and that hence the mass of the recoil system M_{rec} is very close to the value of $\sqrt{s_{aa}}$ and y_{rec} is small.

As an example, Table I gives the recoil mass and rapidity in central $Pb + Pb$ collisions at $\sqrt{s} = 5.5 \times A$ TeV, for $\sqrt{s_{aa}} = 1140$ TeV and when the Centauro fireball mass is $M_{\text{fb}} = 530$ GeV/ c^2 , for different values of Δy_{fb} . From this table it follows that the recoil system is produced in the central rapidity region and, therefore, the secondary particles can be detected by the central detector of any experiment. The composition of the recoil system is unknown.

Strange quark matter fireball. As mentioned earlier gluons in the primary Centauro fireball fragment into $s\bar{s}$ pairs and in this way chemical equilibrium is achieved. The strange

Δy_{fb}	2.0	2.5	3.0	3.5
$M_{\text{rec}}/\sqrt{s_{aa}}$	0.93	0.96	0.97	0.98
y_{rec}	-0.07	-0.04	-0.03	-0.02

TABLE I: Recoil system mass M_{rec} and rapidity y_{rec} in $\sqrt{s} = 5.5 \times A$ TeV $Pb + Pb$ collisions for different values of the rapidity shift due to nuclear stopping Δy_{fb} of the Centauro fireball.

quark number density is given by the equation [16]:

$$n_s = 1.37 \cdot 10^{-3} \text{ GeV}^3 \left(\frac{T}{200 \text{ MeV}} \right) K_2 \left(\frac{m_s}{T} \right), \quad (7)$$

where $K_2(x)$ is a modified Bessel function of the second order. Multiplied by the Centauro fireball volume V_{fb} (4) equation (7) gives the number of $s\bar{s}$ pairs inside the fireball and, hence, the number of emitted K -mesons:

$$N_{\bar{s}} = N(K^+) + N(K^0) = n_s V_{\text{fb}}. \quad (8)$$

Fig. 3 shows the distribution of the number of kaons emitted from the Centauro fireball produced in $\sqrt{s} = 5.5 \times A$ TeV $Pb + Pb$ collisions with $\mu_b = 1.8$ GeV and $T = 130, 190$ and 250 MeV. Before kaons are emitted from the fireball the total number of quarks is

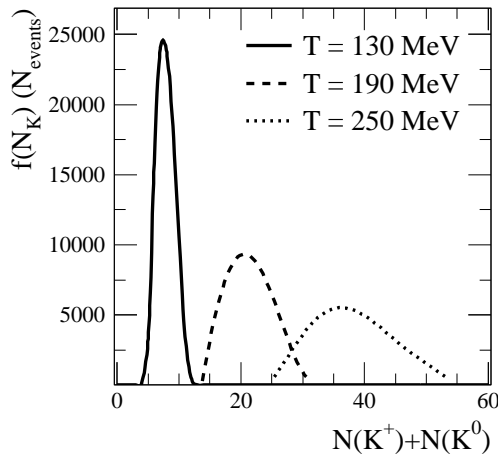


FIG. 3: Number of K^+ and K^0 emitted from the Centauro fireball produced in $\sqrt{s} = 5.5 \times A$ TeV $Pb + Pb$ collisions with $\mu_b = 1.8$ GeV and $T = 130, 190$ and 250 MeV.

$N'_q = 3N_b + 2N_{\bar{s}}$. Hence, the average energy per constituent quark at this stage is

$$\epsilon'_q = \frac{M_{\text{fb}}}{N'_q}. \quad (9)$$

After $2N_{\bar{s}}$ quarks have been emitted as kaons the mass of the remaining SQM fireball is defined by the average quark energy (9) and the number of quarks in the fireball N_q :

$$M'_{\text{fb}} = N_q \epsilon'_q = M_{\text{fb}} \left(1 - \frac{2N_{\bar{s}}}{N_q} \right).$$

The emission of anti-strangeness is described as an isotropic decay of the primary fireball into $N_{\bar{s}}$ kaons and the SQM fireball with the mass M'_{fb} .

Decay of SQM fireball. After emission of kaons the primary Centauro fireball is transformed into a slightly strange quark matter one which can have a long life-time, of the order of 10^{-9} sec [5]. At the final stage of its evolution the SQM fireball decays into baryons and strangelets. The latter are light droplets of strange quark matter with $A > 6$, high strangeness-per-baryon ratio $S/A \approx 1$ and small charge-to-mass ratio $Z/A \approx 0$. For simplicity, only one strangelet is formed in the SQM fireball through random selection of u -, d - and s -quarks among all the quarks of the fireball. If not the complete strangeness content of the SQM fireball is transferred to the strangelet, the remaining s -quarks form strange hyperons. Baryons are formed in the fireball through random selection of sets of three quarks among the quarks of the fireball. Priority is given to the formation of nucleons and all quarks which cannot be incorporated into nucleons produce strange hyperons. The SQM fireball decays isotropically. We use the well-known event generator JETSET [17] to perform further decays of kaons and strange baryons.

General characteristics of Centauro events. Table II shows characteristics of Centauro events in $Pb+Pb$ collisions at $\sqrt{s} = 5.5 \times A$ TeV. At given impact parameter b , temperature T and baryochemical potential μ_b we calculate baryon number N_b , energy density ε , quark number density n_q , volume of fireball V_{fb} , mass of primary fireball M_{fb} , mass of SQM fireball M'_{fb} , strange quark number density n_s and number of emitted kaons $N(K^{+,0})$. For some initial parameters of the model, especially for central collisions ($b = 0$) and high temperature, Centauro events are characterized by a high mass and a large number of kaons. Nuclear collisions with large impact parameters could also produce Centauro-type events but these events are characterized by a smaller strange component.

The Centauro events observed in cosmic ray experiments are characterized by total, or almost total, absence of the photonic component among secondary particles. Since our model is based on the assumption that the primary Centauro fireball consists of u and d quarks and gluons, leading to the suppression of production of \bar{u} and \bar{d} antiquarks as described

b	μ_b	T	N_b	ε	n_q	V_{fb}	M_{fb}	M'_{fb}	n_s	$N(K^{+,0})$
fm	GeV	MeV		GeV/fm ³	fm ⁻³	fm ³	GeV	GeV	fm ⁻³	
0	1.8	130	186	4.3	6.7	83	357	344	0.13	11
		190	186	7.7	9.2	61	466	423	0.48	28
		250	186	13.6	12.5	45	607	515	1.14	50
	1.5	130	186	2.7	4.4	125	334	316	0.13	16
		190	186	5.3	6.5	86	460	402	0.48	40
		250	186	10.4	9.2	60	626	503	1.14	68
5	1.8	130	114	4.3	6.7	51	219	212	0.13	6
		190	114	7.7	9.2	37	286	260	0.48	17
		250	114	13.6	12.5	27	372	315	1.14	31
8	1.8	130	53	4.3	6.7	24	102	98	0.13	3
		190	53	7.7	9.2	17	133	120	0.48	8
		250	53	13.6	12.5	13	173	147	1.14	14

TABLE II: Properties of Centauro events for different fixed values of impact parameter, temperature and baryochemical potential.

previously, it follows that the bulk of secondary hadrons seen in cosmic ray Centauros are baryons.

Kaons emitted from the primary fireball can decay into pions which provide, in turn, an additional source of photons. Overall however the electromagnetic component of such an event is greatly suppressed. Fig. 4 shows the ratio of the hadron multiplicity to the total multiplicity (hadrons + photons) in Centauro events with $\mu_b = 1.8$ GeV and $T = 190$ MeV produced in $\sqrt{s} = 5.5 \times A$ TeV $Pb + Pb$ collisions. The ratio is very close to 1, with mean value $\langle N_h/N_{tot} \rangle = 0.93$, and the deviation of this value from 1 is caused by the electromagnetic particles. Fig. 5 shows the ratio of the summed energy of hadrons to the total energy in the same events. This ratio is also very close to 1, with average value $\langle \sum E_h / \sum E_{tot} \rangle = 0.99$. It should be noted that these ratios depend also on the thermodynamical characteristics of the Centauro fireball, e.g. the higher the temperature, the more kaons and therefore the more photons, are produced and these ratios deviate further from 1.

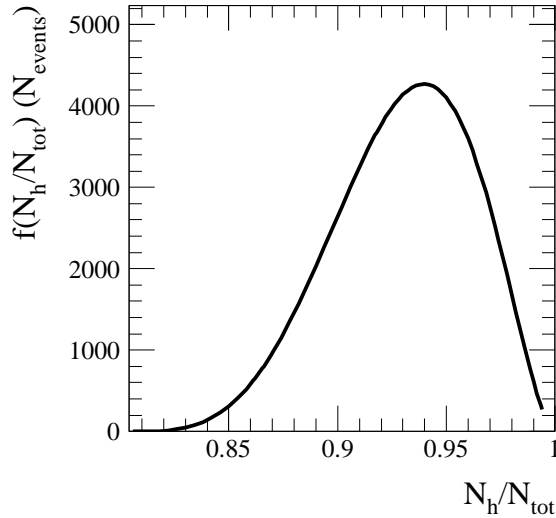


FIG. 4: Ratio of hadron to total multiplicities (hadrons + photons) in Centauro events with $\mu_b = 1.8$ GeV and $T = 190$ MeV produced in $\sqrt{s} = 5.5 \times A$ TeV $Pb + Pb$ collisions.

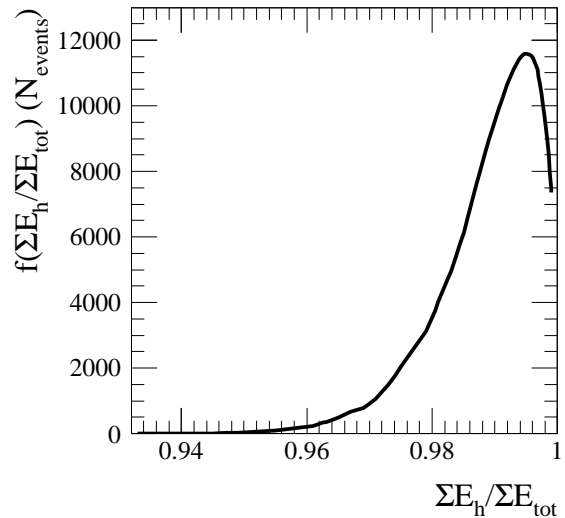


FIG. 5: Ratio of summed hadronic to total energies in Centauro events with $\mu_b = 1.8$ GeV and $T = 190$ MeV produced in $\sqrt{s} = 5.5 \times A$ TeV $Pb + Pb$ collisions.

Secondary particles in events arising from Centauro fireball decay have a larger average transverse momentum in comparison with ordinary hadronic interactions. The mean p_T observed in cosmic rays [1, 2] is $\langle p_T \rangle = 1.75$ GeV/ c . Fig. 6 shows the transverse momentum distribution of hadrons in Centauro events produced in $\sqrt{s} = 5.5 \times A$ TeV $Pb + Pb$ collisions. for three sets of baryochemical potential μ_b and temperature T : $\mu_b = 1.8$ GeV, $T = 190$ MeV; $\mu_b = 1.8$ GeV, $T = 250$ MeV and $\mu_b = 3.0$ GeV, $T = 250$ MeV. The average p_T in such events is $\langle p_T \rangle = 1.34$ GeV/ c , 1.47 GeV/ c and 1.75 GeV/ c respectively. Conventional hadronic events, as predicted by HIJING, have average transverse momentum $\langle p_T \rangle = 0.44$ GeV/ c which is 2 – 4 times smaller than in Centauro events.

The rapidity distribution of decay products of the Centauro fireball clearly depends on the nuclear stopping power. In Fig. 7 the rapidity distributions of secondary particles are shown for three values of the fireball rapidity shift $\Delta y_{fb} = 2.0, 2.5$ and 3.0 . Obviously all secondary particles from the Centauro fireball decay are distributed in the very forward region, as observed in cosmic rays. However, the complete event within which the Centauro fireball is produced contains also the particles of the recoil system which fall in the central

region, $y \approx 0$, according to Table I.

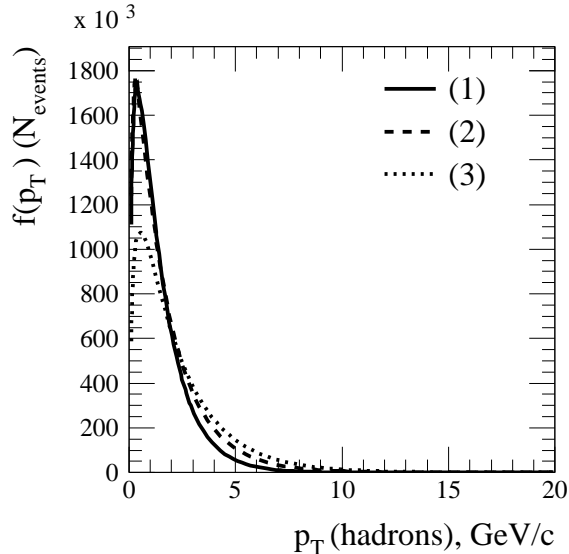


FIG. 6: Transverse momentum distribution of hadrons in Centauro events produced in $\sqrt{s} = 5.5 \times A$ TeV $Pb + Pb$ collisions with $\mu_b = 1.8$ GeV, $T = 130$ MeV (1); $\mu_b = 1.8$ GeV, $T = 190$ MeV (2) and $\mu_b = 3.0$ GeV, $T = 250$ MeV (3).

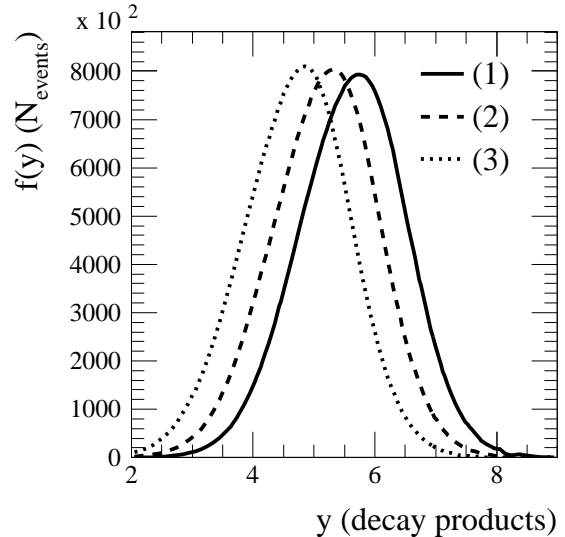


FIG. 7: Rapidity distribution of hadrons in Centauro events produced in $\sqrt{s} = 5.5 \times A$ TeV $Pb + Pb$ collisions for three values of $\Delta y_{fb} = 2.0$ (1), 2.5 (2) and 3.0 (3).

The kinematics of the strangelets which may be produced in the Centauro events are similar to the hadron kinematics. Due to their larger mass, the strangelets have larger transverse momentum. Fig.8 shows the transverse momentum distribution of strangelets formed in the decay of Centauro fireballs produced in $\sqrt{s} = 5.5 \times A$ TeV $Pb + Pb$ collisions for three sets of the thermodynamical parameters, $\mu_b = 1.8$ GeV, $T = 190$ MeV; $\mu_b = 1.8$ GeV, $T = 250$ MeV and $\mu_b = 3.0$ GeV, $T = 250$ MeV. The rapidity distribution of the strangelets is shown in Fig.9 for three values of the fireball rapidity shift $\Delta y_{fb} = 2.0, 2.5$ and 3.0.

II. DETECTION OF CENTAURO EVENTS WITH CASTOR

In this section we present simple calculations of the geometrical detection efficiency of the CASTOR detector at the LHC [18, 19, 20]. The detector will probe the very forward,

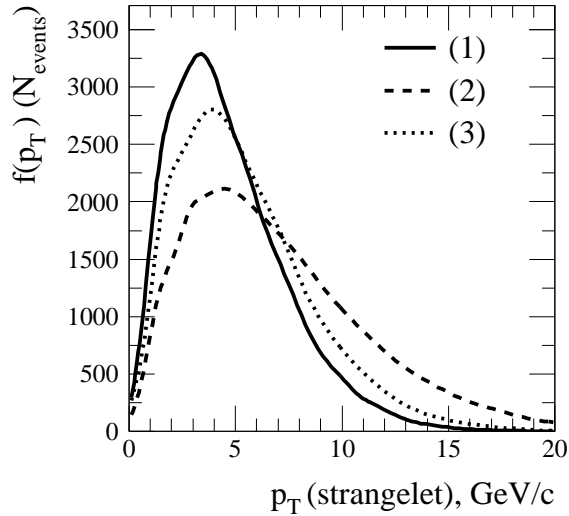


FIG. 8: Transverse momentum distribution of strangelets formed in the decay of Centauro fireballs produced in $\sqrt{s} = 5.5 \times A$ TeV $Pb + Pb$ collisions for $\mu_b = 1.8$ GeV, $T = 130$ MeV (1); $\mu_b = 1.8$ GeV, $T = 190$ MeV (2) and $\mu_b = 3.0$ GeV, $T = 250$ MeV (3).

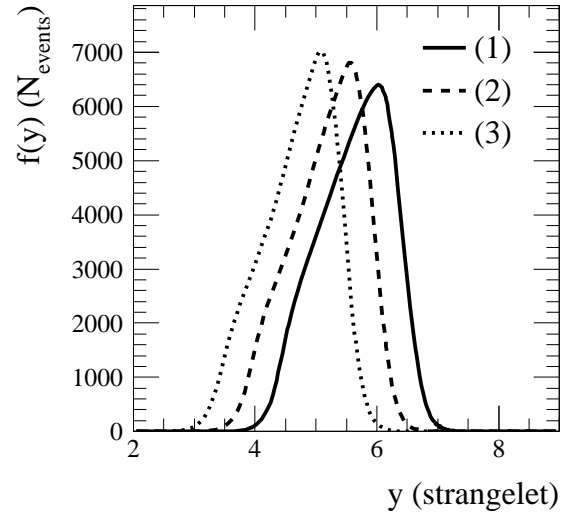


FIG. 9: Rapidity distribution of strangelets formed in the decay of Centauro fireballs produced in $\sqrt{s} = 5.5 \times A$ TeV $Pb + Pb$ collisions for $\Delta y_{fb} = 2.0$ (1), 2.5 (2) and 3.0 (3).

baryon rich region in $\sqrt{s} = 5.5 \times A$ TeV $Pb + Pb$ collisions. It will be installed at ~ 16.4 m from the interaction point, will be azimuthally symmetric around the beam pipe and as close to it as possible. The detector's inner radius will be $R_{in} = 2.8$ cm and its outer radius $R_{out} = 15$ cm, enabling it to cover pseudorapidities $5.6 < \eta < 7.0$. Here we present Monte Carlo calculations of the charged particle and photon multiplicities and electromagnetic and hadronic energies reaching the front face of the detector.

Due to a large lifetime in the rest frame, $\tau \sim 10^{-9}$ sec and a high rapidity, the SQM fireball can decay far apart from the beam interaction point. The decay length of the fireball before its decay depends on the fireball mass and the rapidity shift Δy_{fb} (6). In the Fig. 10 the path length distribution of the fireball is shown for $T = 250$ MeV, $\mu_b = 1.8$ GeV and three values of the rapidity shift $\Delta y_{fb} = 3.0, 2.5$ and 2.0. The detector positions is shown by the vertical solid line. As it is seen, the significant number of SQM fireballs decays beyond the detector, i.e. their decay products will not be detected. Only K -mesons which emitted from

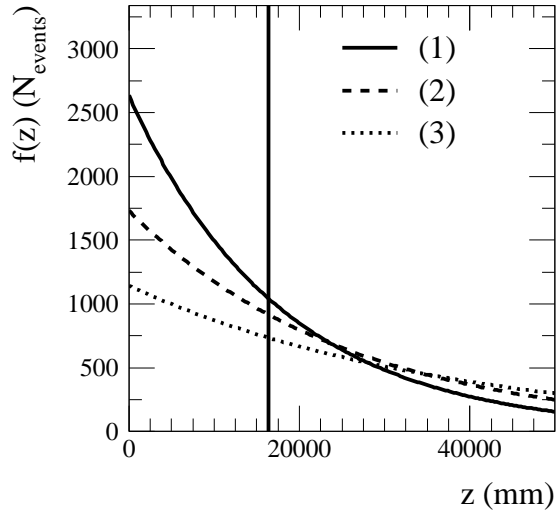


FIG. 10: Decay length of the SQM fireball at $T = 250$ MeV, $\mu_b = 1.8$ GeV and $\Delta y_{\text{fb}} = 3.0, 2.5, 2.0$. The vertical line at $z = 16.4$ m shows the detector positions.

the primary Centauro fireball at the initial stage of its evolution can be detected.

The detection of secondary particles of the Centauro events also strongly depends on the parameters of the model, namely the thermodynamical variables μ_b and T which influence the mass of the fireball and the fireball rapidity shift due to nuclear stopping Δy_{fb} . We compare the ability of CASTOR to detect Centauro fireballs produced at different T and fixed μ_b and Δy_{fb} , as well as at different Δy_{fb} and fixed thermodynamical parameters. Fig. 11 shows the charged hadron multiplicity distribution at the detector for fixed $\Delta y_{\text{fb}} = 2.5$ and $\mu_b = 1.8$ GeV and three values of the fireball temperature $T = 130, 190$ and 250 MeV. The dependence of the charged hadron multiplicity on the rapidity shift for fixed $\mu_b = 1.8$ GeV and $T = 250$ MeV is shown in Fig. 12: the curves correspond to $\Delta y_{\text{fb}} = 2.0, 2.5$ and 3.0 . The shape of these distributions is affected by the decay length distribution shown in Fig. 10. The sharp peaks at small multiplicity corresponds to the events when the SQM fireball decays behind the detector, and only K -mesons contribute to the detected multiplicity.

The number of detected charged hadrons for each set of parameters has to be compared to the total number of charged hadrons generated in the Centauro event. The geometrical detection efficiency of the detector for different values of the model parameters is tabulated in Table III. The fourth column gives the average geometrical efficiency of charged hadron detection $e_{\text{ch.had.}}$ in terms of μ_b , T and Δy_{fb} . The charged hadron multiplicity of Centauro-type events in the detector is rather small, not more than 120 with mean values $30 - 60$. The photon multiplicity is much smaller as can be seen from Fig. 4.

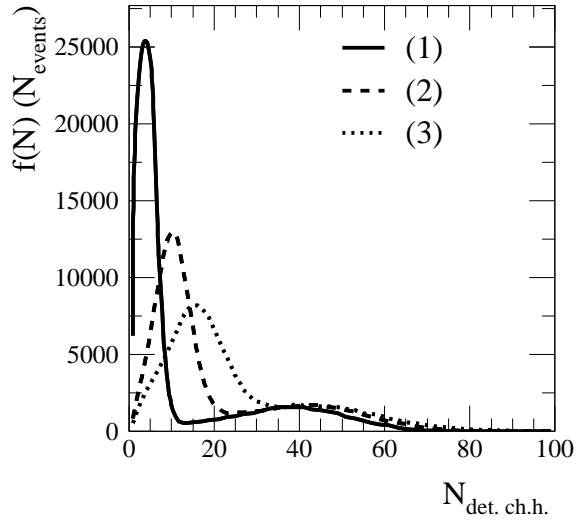


FIG. 11: Charged hadron multiplicity in the detector for Centauro events produced in $\sqrt{s} = 5.5 \times A$ TeV $Pb + Pb$ collisions for fixed $\Delta y_{fb} = 2.5$, $\mu_b = 1.8$ GeV and $T = 130$ (1), 190 (2) and 250 MeV (3).

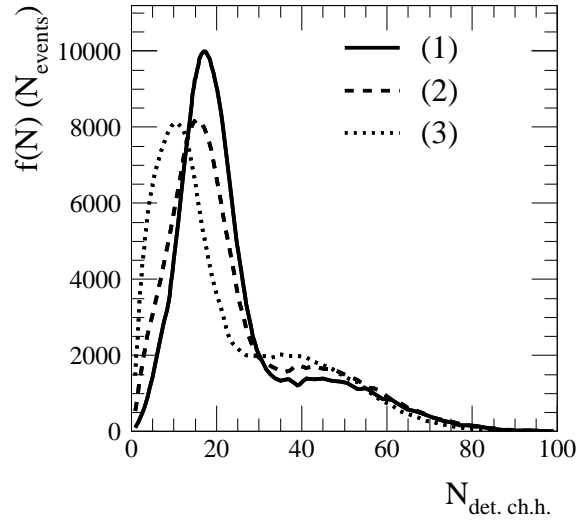


FIG. 12: Charged hadron multiplicity in the detector for Centauro events produced in $\sqrt{s} = 5.5 \times A$ TeV $Pb + Pb$ collisions for fixed $\mu_b = 1.8$ GeV, $T = 250$ and $\Delta y_{fb} = 2.0$ (1), 2.5 (2) and 3.0 (3).

μ_b , GeV	T , MeV	Δy_{fb}	$e_{ch.had.}$	$e_{str.}$
1.8	130	2.5	0.38	0.67
1.8	190	2.5	0.42	0.57
1.8	250	2.5	0.46	0.46
1.8	250	2.0	0.42	0.61
1.8	250	3.0	0.35	0.36
3.0	250	2.5	0.39	0.45

TABLE III: Geometrical detection efficiency e of charged hadrons and strangelets in terms of μ_b , T and Δy_{fb} .

The small multiplicity of the Centauro events is in sharp contrast to what is expected for conventional nuclear collisions where the multiplicity is calculated to be of the order of a few thousand. Fig. 13 shows the charged hadron multiplicity detected by CASTOR in conventional $\sqrt{s} = 5.5 \times A$ TeV $Pb + Pb$ collisions with impact parameters $0 < b < 5$ fm

as predicted by HIJING. The multiplicity in the conventional events is several times higher

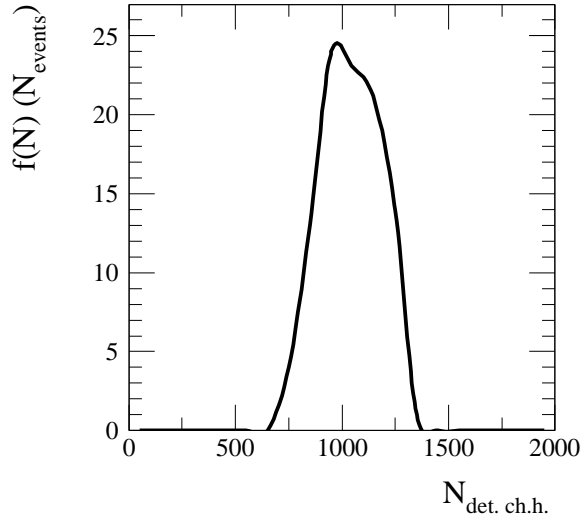


FIG. 13: Charged hadron multiplicity in the detector in conventional $\sqrt{s} = 5.5 \times A$ TeV $Pb + Pb$ collisions as predicted by HIJING.

than that in the Centauro-type events, with an average detected multiplicity of 1000 which is about 20 times that in Centauro events.

Because of their larger mass strangelets are boosted forward more than ordinary hadrons are. Therefore strangelets have a tendency to fly closer to the beam. The distribution of the radius of strangelet hits on the detection plane for strangelets formed in the decay of Centauro fireballs produced in $\sqrt{s} = 5.5 \times A$ TeV $Pb + Pb$ collisions with $\mu_b = 1.8$ GeV, $T = 250$ MeV and $\Delta y_{fb} = 2.5$ is shown in Fig. 14. The shaded area corresponds to the

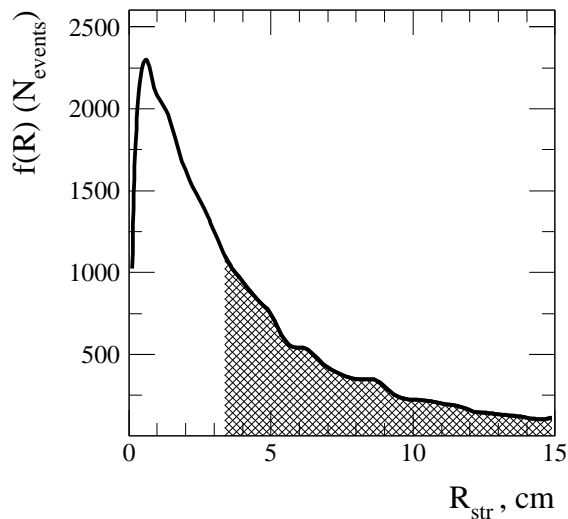


FIG. 14: Distribution of hit radius on the detection plane of strangelets formed in the decay of Centauro fireballs produced in $\sqrt{s} = 5.5 \times A$ TeV $Pb + Pb$ collisions with $\mu_b = 1.8$ GeV, $T = 250$ MeV and $\Delta y_{fb} = 2.5$. Shaded area corresponds to the detector surface.

detector surface. The geometrical efficiency of strangelet detection $\epsilon_{\text{str.}}$ for different values of the model parameters is given in the last column of Table III.

Results obtained for somewhat different detector configurations and model parameters have been presented in [6, 21].

Conclusions

We presented quantitative simulated results on the observation of Centauro events in heavy ion collisions at LHC energies. The phenomenological model of Centauro events originally introduced in [4, 5] gives a transparent explanation of such events. On the basis of this model we constructed the quantitative model and the event generator CNGEN which provides a tool to estimate the geometrical detection efficiency of Centauro events and associated strangelets.

The possibility to observe Centauro events depends strongly on the parameters of the model such as thermodynamical characteristics and the nuclear stopping power.

The signatures for observation of Centauro events with the CASTOR detector can be summarized as follows:

- small detected charged particle multiplicity, $\langle N_{\text{ch. h.}} \rangle = 50$ compared to $\langle N_{\text{ch. h.}} \rangle = 1000$ in conventional hadronic events;
- significant predominance of the detected hadron multiplicity which can be characterized by the average hadron-to-all particles ratio $\langle N_h/N_{\text{tot}} \rangle > 0.9$ while this ratio is equal to $\langle N_h/N_{\text{tot}} \rangle = 0.6$ in conventional hadronic events;
- significant predominance of the detected hadron energy deposited in the detector, $\langle \sum E_h / \sum E_{\text{tot}} \rangle = 0.99$ compared to $\langle \sum E_h / \sum E_{\text{tot}} \rangle = 0.80$ in conventional hadronic events;
- large average transverse momentum, $\langle p_T \rangle > 1 \text{ GeV}/c$ compared to $\langle p_T \rangle = 0.44 \text{ GeV}/c$ in conventional hadronic events.

The model affords the possibility of strangelet production in the decay of the Centauro fireball. If such objects exist and behave according to the model, for $A > 6$ their geometrical

detection efficiency in CASTOR would be about 40 – 60%. The geometrical detection efficiency of the other secondaries of the Centauro events is also satisfactory.

This work was partly supported by Polish State Committee for Scientific Research grant No. 2P03B 011 18 and SPUB-M/CERN/P-03/DZ 327/2000. The authors would like to thank Zbigniew Włodarczyk for useful remarks.

The source code of the event generator CNGEN can be obtained by request from `kharlov@mx.ihep.su`.

-
- [1] C.M.G. Lattes, Y. Fugimoto and S. Hasegawa, *Phys. Rep.* **65** (1980) 151;
 - [2] Chacaltaya and Pamir Collaboration, Contributions to 23rd ICRC (Calgary, 19–30 July, 1993), ICRR-Report-295-93-7 (1993);
 - [3] A.D. Panagiotou et al., *Z. Phys.* **A333** (1989), 355.
 - [4] A.D. Panagiotou et al., *Phys. Rev.* **D45** (1992) 3134.
 - [5] M.N. Asprouli, A.D. Panagiotou and E. Gładysz-Dziaduś, *Astropart. Phys.* **2** (1994) 167.
 - [6] E. Gładysz-Dziaduś, Report INP, Kraków No 1879/PH; hep-ph/0111163; to be publ. in *Phys. Part. Nucl.* #1 **34** 2003.
 - [7] ALICE Technical Proposal, CERN/LHCC/95-71.
 - [8] CMS Technical Proposal, CERN/LHCC/94-38.
 - [9] E. Gładysz-Dziaduś and A.D. Panagiotou, Proc. Int. Symp. on Strangeness & Quark Matter, Krete, 1994, eds. G. Vassiliadis et al, World Scientific, 1995, p 265; Internal note ALICE/PHY/95-18.
 - [10] O.P. Theodoratou and A.D. Panagiotou, *Astropart. Phys.* **13** (2000) 173.
 - [11] C. Greiner, D.H. Rischke, H. Stöcker and P. Koch, *Phys. Rev.* **D38** (1988) 2797.
 - [12] B. Müller, Preprint DUKE-TH-92-36, e-print hep-th/9211010.
 - [13] J.W. Harris and B. Müller, Preprint DUKE-TH-96-105, e-print hep-ph/9602235.
 - [14] M. Gyulassy and X.-N. Wang, *Comput. Phys. Commun.* **83** (1994) 307; Preprint LBL-34346; e-print nucl-th/9502021.
 - [15] K. Werner, *Phys. Rept.* **232** (1993) 87.

- [16] T.S. Biro and J. Zimanyi, Nucl. Phys. **A395** (1983) 241.
- [17] T. Sjöstrand, PYTHIA 5.7 and JETSET 7.4 physics and manual, Comp. Phys. Comm. **82** (1994) 74.
- [18] A.L.S. Angelis and A.D. Panagiotou, J. Phys. G: Nucl. Part. Phys. **23** (1997) 2069.
- [19] A.L.S. Angelis et al, hep-ex/9901038 and in Proc. XXVIII Int. Symp. on Multiparticle Dynamics, Delphi, Greece, 1998, eds. N.G.Antoniou et al., World Scientific, Singapore 1999, p 134.
- [20] A.L.S. Angelis et al, Int. note ALICE/CAS 1997-07.
- [21] E. Gładysz-Dziadus et al., Proc. 3rd Int. Conf. on Physics and Astrophysics of Quark-Gluon Plasma, Jaipur 1997, eds. B.C. Sinha et al., Narosa Publishing House, New Delhi 1998, p. 554;